Journal of Energy Storage 86 (2024) 111418

Contents lists available at ScienceDirect

Journal of Energy Storage

journal homepage: www.elsevier.com/locate/est

Short Communication

Innovative lead-carbon battery utilizing electrode-electrolyte assembly inspired by PEM-FC architecture

Rodrigo F.B. de Souza *, Gabriel A. Silvestrin, Felipe G. Da Conceição, Victoria A. Maia, Larissa Otubo, Almir O. Neto, Edson P. Soares

Instituto de Pesquisas Energéticas e Nucleares, IPEN-CNEN/SP, Cidade Universitária, Av. Professor Lineu Prestes, 2242, São Paulo 05508-900, SP, Brazil

ARTICLE INFO

Keywords:
Carbon-lead acid battery
Flexible lead battery
Cyclic voltammetry
Fuel cell
Pb/C

ABSTRACT

This study explores the innovative integration of a lead-carbon battery with an electrode-electrolyte assembly inspired by Proton Exchange Membrane Fuel Cell (PEM-FC) architecture. The lead-carbon material, synthesized with a 40 % mass ratio using the Flash Joule Heating Method, exhibits predominant Pb^0 and PbO phases, as observed in lattice parameter fringes, with additional detection of the PbO_2 phase. The resulting Carbon-Lead Acid Battery (CLAB) demonstrates a specific capacity of 11.2 mAh g^{-1}. The incorporation of carbon enhances nanoparticle stability, yielding a highly stable battery performance over 100 cycles, with discharge potential variations of <2 %. This innovative CLAB assembly not only showcases stable performance and also introduces the potential for constructing flexible lead batteries, expanding technological applications. The study provides comprehensive insights into the synthesis, performance, and prospects of this novel lead-carbon battery architecture, emphasizing its significance in the realm of energy storage solutions.

1. Introduction

The lead-acid battery (LAB) technology, although originating in the second half of the 19th century, continues to play an important role in the global rechargeable battery market, widely applied in the automotive and industrial sectors due to its characteristics of low cost, mature manufacturing processes, and sustainable recycling [1,2]. However, for new applications requiring a high-rate partial state of charge, such as in hybrid vehicles and specific grid energy storage applications, the performance and lifespan of the lead-acid battery are significantly limited due to negative plate sulfation [3,4].

The thickness of electrodes in commercial LAB batteries is typically in the order of millimeters, which can constrain battery performance due to poor mass transfer within the electrode [1]. The charge transfer reaction in a lead-acid battery is expressed as follows:

$$Pb(s) + PbO_2(s) + 4H^+(aq) + 2SO_4^{2-}(aq) \leftrightarrow 2PbSO_4(s) + 2H_2O(l) \quad (1)$$

The efficiency of active material utilization is easily limited by mass transfer and electrode electrical conductivity due to the non-conductivity and insolubility of the discharge product ($PbSO_4$) and the insufficient hydrogen sulfate anions from the electrolyte in the electrode [2,5]. Key requirements for modern batteries include high power and charge capacities, long lifespan, weight reduction and security. Currently, most efforts to improve LAB involve replacing heavy lead grids with lighter alternatives, such as those based on steel, copper, titanium, and aluminum [6,7], and decrease the H_2 liberation [8]. Recent studies are now focusing on replacing metal alloys with lead-carbon composites [9–11].

This battery technology is commonly referred to as carbon-lead acid battery (CLAB) and is currently the only viable, mass-produced technology available for start-stop systems and basic micro-hybrid vehicles. It is expected that CLAB technology will play a significant role in grid energy storage applications in the future [1,4,12].

The use of nano-Pb/C composite materials demonstrates higher conductivity and lower ion transfer resistance [10]. Lead-carbon materials for CLAB exhibit electrochemical characteristics similar to metallic lead in the same potential ranges as lead-acid batteries. Moreover, it has been shown that carbon does not participate in the electrochemical process but enhances the corrosion and stability of lead, inhibiting the formation of species that deteriorate the discharge characteristics of the positive electrode, such as large clusters of lead sulfate [4,9].

According to Yolshina [9], a promising solution to creating a new generation of lead-acid batteries would be to obtain radically new

* Corresponding author.
E-mail address: souza.rfb@gmail.com (R.F.B. de Souza).

https://doi.org/10.1016/j.est.2024.111418
Received 9 January 2024; Received in revised form 28 February 2024; Accepted 20 March 2024
Available online 23 March 2024

nanocomposites and lead alloys with a high carbon content. Another electrochemical device that could contribute to this new generation of lead batteries is the proton exchange membrane fuel cell [13]. In these devices, the active metal is deposited in a layer of a few micrometers, laid upon a backbone of carbon cloth, where lead nanoparticles can be deposited, increasing stability and reducing weight. The thin layers of active material from the anodic and cathodic electrons are then separated by a proton-exchange membrane, which facilitates the transport of H^+ and plays an essential role in efficiently transporting this proton through a solid medium, thus avoiding gas evolution. This electrode structure with a polymeric electrolyte enables the production of a flexible device, giving engineers the possibility to construct or accommodate it in various types of spaces. In this context, in this work, the construction of a CLAB using the architecture of a fuel cell has been studied.

2. Experimental

A Pb/C material with a composition of 40 % was synthesized using the Flash Joule Heating Method (FJHM) developed in our laboratory. In this process, appropriate quantities of the metal precursor PbO (Aldrich) and HNO_3 (0.1 mol L^{-1}) were mixed in a 40:60 (m/m) ratio of metal precursor to Vulcan XC 72 carbon support within a graphite crucible. The crucible was then sealed and exposed to 50 discharge cycles at 100 C per discharge, at 65 V, for a total duration of 60 s. Following this, the resulting FJHM-Pb/C material underwent subsequent characterization.

The obtained material was characterized through X-ray diffraction (XRD) using a Rigaku Miniflex II diffractometer equipped with a Cu Kα source (λ = 1.54056 Å) at a 2θ range spanning from 20° to 90°, employing a step size of 0.02° and a scan duration of 2.0 s per step. Transmission Electron Microscopy (TEM) analysis was carried out employing a JEOL electron microscope model JEM-2100.

Cyclic voltammetry measurements were conducted at a temperature of 25 °C, employing an Autolab PGSTAT 302 potentiostat/galvanostat. The working electrode comprised a carbon vitreous material with a deposited porous ultrathin layer [14]. The reference electrode used was the Ag/AgCl (3.0 mol L^{-1} KCl), while the counter electrode took the form of a platinum (Pt) plate. These electrochemical analyses were performed within 0.5 mol L^{-1} H_2SO_4 solutions saturated with nitrogen (N_2).

Battery cell experiments were carried out using a Pb/C-nafion-Pb/C electrode setup. Pb/C electrodes were prepared with 5 mg of Pb/C per cm^2 on electrodes with a 5.0 cm^2 area (Fig. 1a). The material was mixed with 5 % by mass of Nafion 520 and 5 μL of isopropyl alcohol, which was sonicated for 15 min. Subsequently, this ink was applied to a treated carbon cloth backbone, and the separator and electrolyte were applied using the Nafion® 115 membrane, and pressed at 125 °C for 2.0 min at 125 kgF cm^{-2} (Fig. 1b).

The membrane electrode assembly (MEA) was carefully packed and positioned within a solution containing 0.5 mol L^{-1} sulfuric acid (Fig. 1c-d), serving as both the cathode and anode environments. Subsequently, following assembly, the experimental cells underwent an activation process characterized by the application of a voltage of 2.0 V for a duration of 2 h. Galvanostatic charge and discharge tests were then conducted utilizing a PARSTAT3000A potentiostat, employing varying rates of 0.5, 1, 5, and 10 C g^{-1}, with a potential span ranging from 0.0 to 2.0 V. Each rate was subjected to 5 cycles, and capacity rate tests were carried out in duplicate. Furthermore, cyclic stability testing, executed at a charge of 10 C g^{-1}, was performed at room temperature, spanning between the battery's open circuit voltage and 0.0 V, over a span of 100 cycles in duplicate.

3. Results and discussion

In the TEM images depicted in Fig. 1, it is evident that lead particles assume an elongated and slender morphology, with highlighted agglomerated regions (Fig. 2a). The distinct corners observed in the Pb/C nanoparticles can be attributed to a rapid and forced reduction process induced by the electron cascade resulting from discharges during synthesis. In the corresponding histogram (Fig. 2b), an average length size of approximately 46 nm for the nanoparticles was observed. In Fig. 2c, the lattice fringe of the lead crystal is clearly visible at high magnification, with fringe sizes of 0.285 nm and 0.400 nm observed. These measurements correspond closely to the data provided by JCPDS 04-0686 and 05-561 for Pb and PbO, respectively, indicating the presence of these two phases within the same nanoparticle. The existence of these two phases is confirmed by X-ray diffraction (XRD) analysis in Fig. 2d.

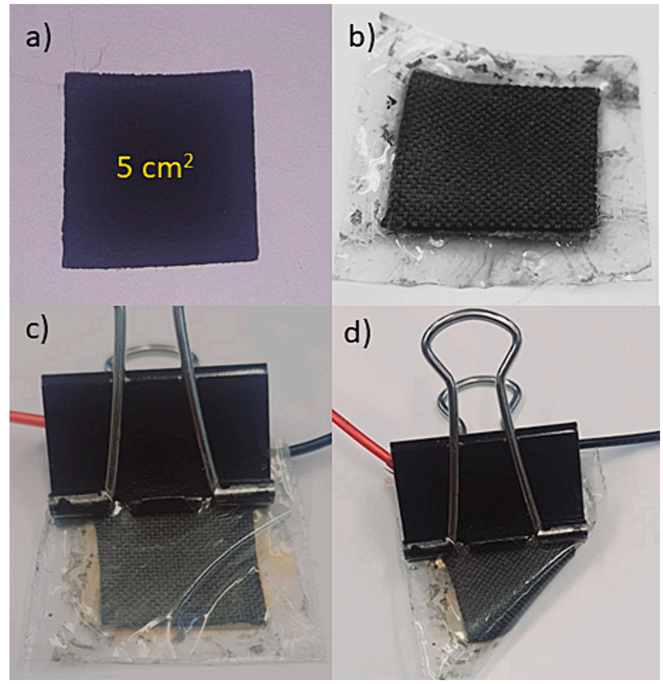

Fig. 1. a) Pb/C electrode, b) Membrane electrode assemble (MEA), c-d) Flexible device.

The X-ray diffraction (XRD) analysis of FJHM-Pb/C revealed distinct patterns, with peaks at 2θ = 22° and 38° corresponding to characteristic structures of amorphous carbon with low crystallinity [15]. Additionally, three phases associated with lead and its oxides were discerned. The diffraction patterns exhibited prominent peaks at 2θ angles around 31.3°, 36.4°, 52.4°, 62.2°, and 67°, corresponding to Pb (JCPDS 04-0686). Peaks at 28.7°, 32°, 42°, 44.8°, 45.3°, 48.6°, 54.8°, and 60° were attributed to PbO (JCPDS 05-561). Furthermore, peaks at 25.3° and 49.2° were assigned to PbO_2 (JCPDS 41-1492). This suggests that the reduction process was not complete. It is noteworthy that in high-resolution transmission electron microscopy (HRTEM), no planes related to the PbO_2 phase were observed, only the lattice fringes of Pb and PbO. According to Li and co-workers [16], the presence of lead in the form of nanoparticles enhances the stability and lifespan of the battery, primarily by preventing the irreversible growth of crystals on the redox surface of the electrode.

In Fig. 3, the cyclic voltammogram of 40 % Pb/C is depicted, revealing a combination of the typical carbon profile with distinctive lead peaks marked by the $PbSO_4/PbO_2$ redox couple at 1.1 and 0.9 V. The transition from $PbSO_4$ to PbO_2 aligns closely with the oxygen evolution, as described by Visscher [17].

Fig. 4a illustrates the cell potential of the CLAB cell versus discharge current using Nafion as a separator and polymer electrolyte membranes. In this curve, the open circuit voltage of the cell is approximately 2.0 V, reaching the proton diffusion limit at around 0.3 V with a current of 2.5 mA mg_{Pb}^{-1} at room temperature. The maximum power density achieved

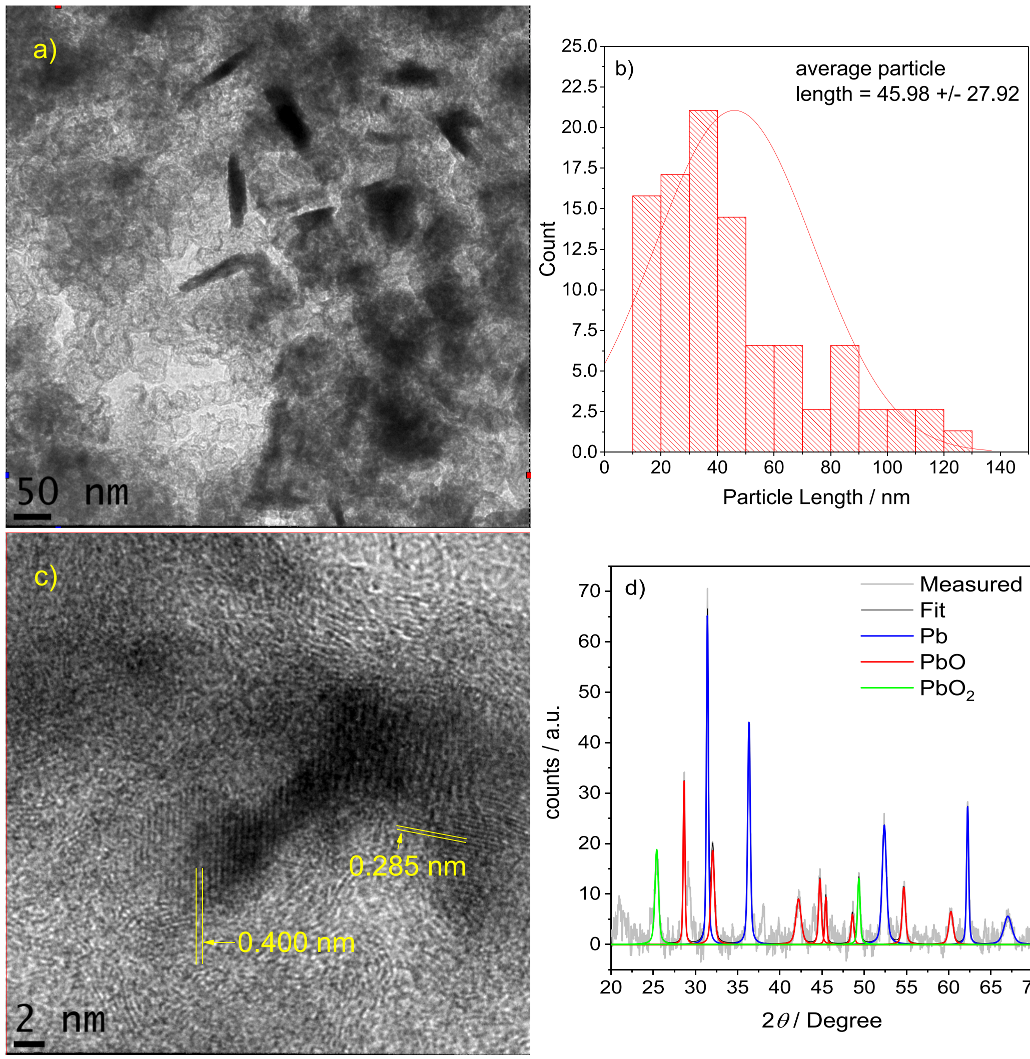

Fig. 2. a) Transmission electron microscopy, b) Histogram with particle size distribution, c) Lattice fringe of the lead PbO crystal, and d) XRD pattern of FJHM-Pb/C.

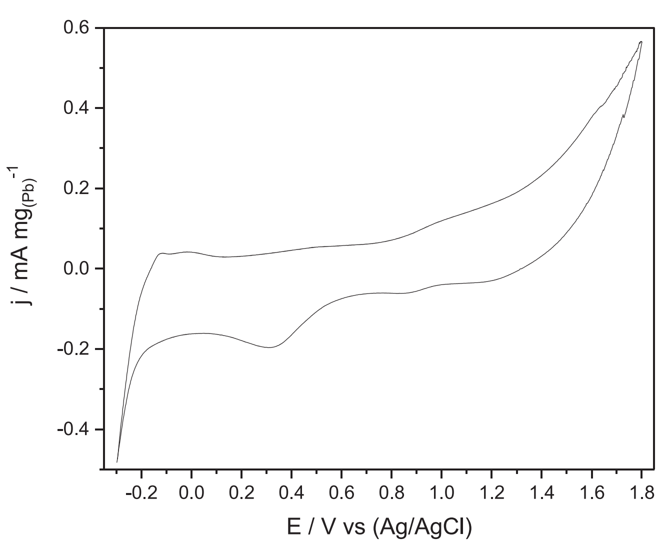

Fig. 3. Cyclic voltammetry in H_2SO_4 0.5 mol L^{-1} v = 10 m s^{-1} for Pb/C with a 40 % mass ratio.

by this cell was 1.7 mW mg_{Pb}^{-1}.

At a charge and discharge rate of 10 mA mg^{-1}, the typical discharge profile [13] is presented in Fig. 4b, where the termination voltage is 1.83 V. The discharge specific capacity of the RHPC battery is 11.2 mAh g^{-1}. A rate capability test (RCT) was conducted (Fig. 4c), revealing capacities ranging from 13.5 to 18.0 mAh g^{-1}, demonstrating a difference of <35 % for the highest battery drain, indicating the device's robustness.

To assess the performance of the CLAB cell in a deeply charge/discharge process, the formed cells and cells after deep charge/discharge for 100 cycles were analyzed at a discharge rate of 10 mA g^{-1} (Fig. 5), demonstrating good stability throughout the entire experiment. It is noteworthy that the capacity remains quite stable at ~13.8 mAh g^{-1}. Additionally, no hydrogen evolution was observed during the experiment.

The cycle performance of the 2.1 V carbon lead-acid cell is illustrated in Fig. 4 through high-rate partial-state-of-charge (HRPSoC) testing, showcasing a discharge cut-off voltage of 2.03 V with approximately 1 % variation over 100 cycles. This suggests that the formation of $PbSO_4$ is not being favored. According to Zhong and co-workers [10], the incorporation of nano-lead in the composite material enhances reactivity, increases the affinity between lead and carbon, and establishes a conductive connection among active material particles. This improvement contributes to enhanced conductivity and electrochemical activity in the electrode while also suppressing the formation of large $PbSO_4$

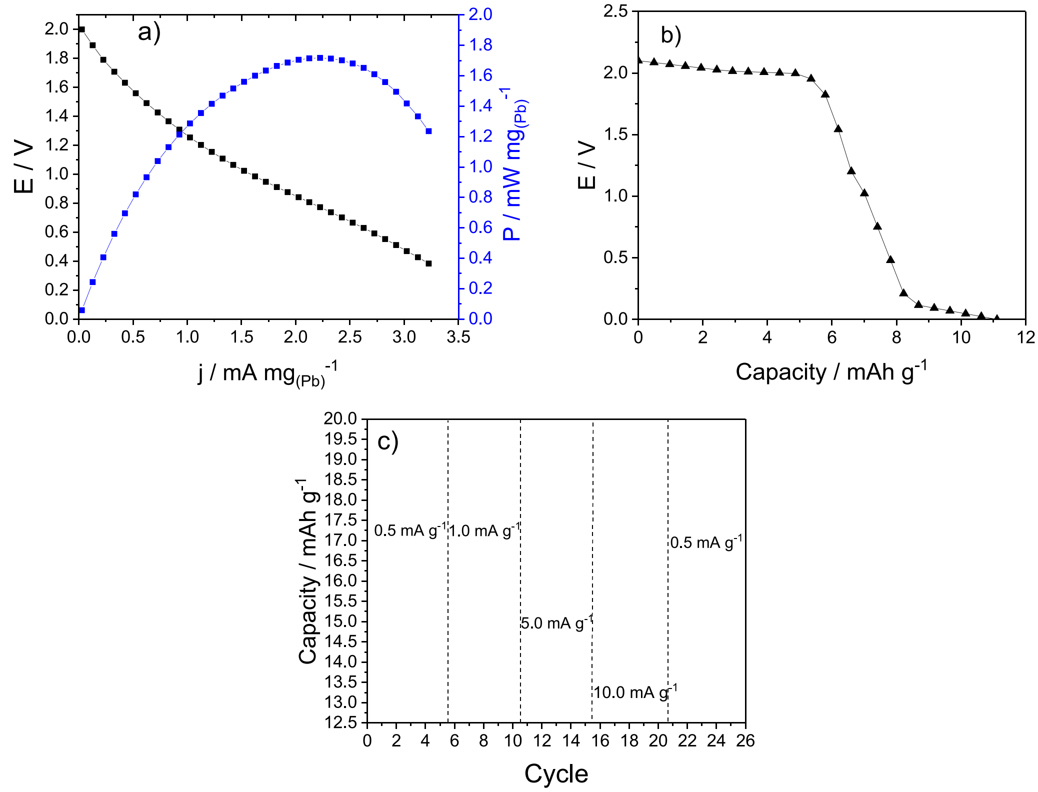

Fig. 4. a) Polarization and power curve; b) discharge at 10 mA g^{-1}, c) Specific discharge capacity, using different charge/discharge rates for Pb/C with a 40 % mass ratio.

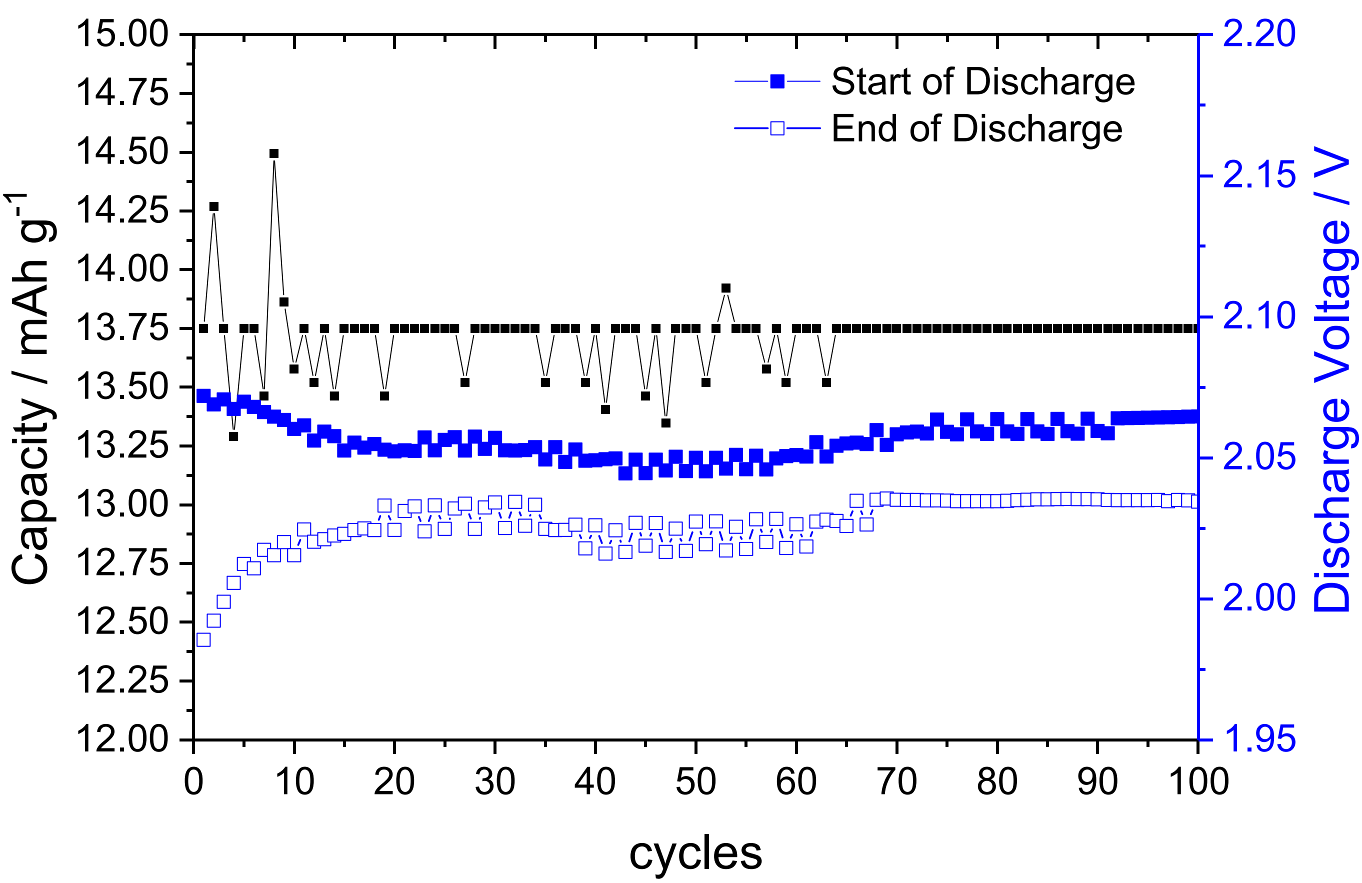

Fig. 5. Charge/discharge process for 100 cycles for Pb/C with a 40 % mass ratio.

crystals [18].

The effect of adding carbon materials to LABs has also been reported by Pavlov et al. [19], indicating that the additive is available to reduce the average pore size of the negative active material, potentially inhibiting the roughness of $PbSO_4$ particles. In the present case, since we are dealing with lead nanoparticles rather than macroscopic plates, the pores, if present, are much smaller in size compared to Pavlov's work, thus inhibiting the fixation of $PbSO_4$. Additionally, nanoparticles offer the possibility of non-planar diffusion, further complicating the anchoring of $PbSO_4$. Furthermore, with high conductivity, carbon can enhance the electrode's conductivity and further drive the entire cycle process, hence providing greater stability [20].

4. Conclusion

The construction of a Lead-Carbon battery using the MEA architecture of a PEM-FC has demonstrated significant promise and stability. Utilizing Pb/C with a 40 % mass ratio, synthesized through the Flash Joule Heating Method, revealed predominant Pb0 and PbO phases, evident in the lattice parameter fringes, along with the detection of the PbO_2 phase. The Carbon-Lead Acid Battery exhibited a specific capacity of 11.2 mAh g^{-1}. The incorporation of carbon into the lead structure not only enhanced the stability of the nanoparticles, however also resulted in a highly stable battery performance over 100 cycles, with discharge potential variations of <2 %. Moreover, this CLAB assembly provides the potential for constructing flexible lead batteries, thereby expanding the scope of technological applications. The successful integration of PEM-FC architecture into CLAB technology opens avenues for innovative and flexible energy storage solutions.

CRediT authorship contribution statement

Rodrigo F.B. de Souza: Methodology, Investigation, Formal analysis, Data curation, Conceptualization. **Gabriel A. Silvestrin:** Methodology. **Felipe G. Da Conceição:** Methodology. **Victoria A. Maia:** Investigation. **Larissa Otubo:** Methodology, Investigation. **Almir O. Neto:** Writing – original draft, Supervision, Investigation, Funding acquisition, Data curation, Conceptualization. **Edson P. Soares:** Writing – original draft, Methodology, Investigation, Formal analysis, Data curation, Conceptualization.

Declaration of competing interest

The authors declare that they have no known competing financial interests or personal relationships that could have appeared to influence the work reported in this paper.

Data availability

Data will be made available on request.

Acknowledgments

This research was funded by CAPES, CNPq (350514/2023-2, 302709/2020-7) and FAPEAM (012/2021 – POSGRAFE) for financial support.

References

[1] A. Jaiswal, S.C. Chalasani, The role of carbon in the negative plate of the lead–acid battery, J. Energy Storage 1 (2015) 15–21, https://doi.org/10.1016/j.est.2015.05.002.
[2] S. Mandal, S. Thangarasu, P.T. Thong, S.-C. Kim, J.-Y. Shim, H.-Y. Jung, Positive electrode active material development opportunities through carbon addition in the lead-acid batteries: a recent progress, J. Power Sources 485 (2021) 229336, https://doi.org/10.1016/j.jpowsour.2020.229336.
[3] X. Xu, J. Liu, Q. Zhang, H. Wang, A facile approach to suppress the sulfation in lead acid batteries using N-doped carbon derived from chitosan, Mater. Lett. 247 (2019) 29–31, https://doi.org/10.1016/j.matlet.2019.03.055.
[4] K. Yanamandra, D. Pinisetty, N. Gupta, Impact of carbon additives on lead-acid battery electrodes: a review, Renew. Sust. Energ. Rev. 173 (2023) 113078, https://doi.org/10.1016/j.rser.2022.113078.
[5] H.A. Catherino, F.F. Feres, F. Trinidad, Sulfation in lead–acid batteries, J. Power Sources 129 (1) (2004) 113–120, https://doi.org/10.1016/j.jpowsour.2003.11.003.
[6] P.P. Lopes, V.R. Stamenkovic, Past, present, and future of lead–acid batteries, Science 369 (6506) (2020) 923–924, https://doi.org/10.1126/science.abd3352.
[7] Y. Zhang, C.-g. Zhou, J. Yang, S.-c. Xue, H.-l. Gao, X.-h. Yan, et al., Advances and challenges in improvement of the electrochemical performance for lead-acid batteries: a comprehensive review, J. Power Sources 520 (2022) 230800, https://doi.org/10.1016/j.jpowsour.2021.230800.
[8] F. Wang, C. Hu, M. Zhou, K. Wang, J. Lian, J. Yan, et al., Research progresses of cathodic hydrogen evolution in advanced lead–acid batteries, Sci. Bull. 61 (6) (2016) 451–458, https://doi.org/10.1007/s11434-016-1023-0.
[9] L.A. Yolshina, V.A. Yolshina, A.N. Yolshin, S.V. Plaksin, Novel lead-graphene and lead-graphite metallic composite materials for possible applications as positive electrode grid in lead-acid battery, J. Power Sources 278 (2015) 87–97, https://doi.org/10.1016/j.jpowsour.2014.12.036.
[10] J. Zhong, J. Gu, K.-d. Zhu, X.-r. Wang, S.-l. Wang, Quasi-solid synthesis of nano-Pb/C composites for enhanced performance of lead-acid battery, J. Energy Storage 47 (2022) 103535, https://doi.org/10.1016/j.est.2021.103535.
[11] E. Ebner, D. Burow, J. Panke, A. Börger, A. Feldhoff, P. Atanassova, et al., Carbon blacks for lead-acid batteries in micro-hybrid applications – studied by transmission electron microscopy and Raman spectroscopy, J. Power Sources 222 (2013) 554–560, https://doi.org/10.1016/j.jpowsour.2012.08.089.
[12] D.G. Enos, S.R. Ferreira, H.M. Barkholtz, W. Baca, S. Fenstermacher, Understanding function and performance of carbon additives in lead-acid batteries, J. Electrochem. Soc. 164 (13) (2017) A3276, https://doi.org/10.1149/2.1031713jes.
[13] A. Alaswad, A. Omran, J.R. Sodre, T. Wilberforce, G. Pignatelli, M. Dassisti, et al., Technical and commercial challenges of proton-exchange membrane (PEM) fuel cells, Energies 14 (2021) 144, https://doi.org/10.3390/en14010144.
[14] R.F.B. De Souza, É.T. Neto, M.L. Calegaro, E.A. Santos, H.S. Martinho, M.C. dos Santos, Ethanol electro-oxidation on Pt/C electrocatalysts: an "in situ" Raman spectroelectrochemical study, Electrocatalysis 2 (1) (2011) 28–34, https://doi.org/10.1007/s12678-010-0031-0.
[15] C. Hu, J. Li, Q. Li, T. Lan, J. Zhang, S. Zhou, et al., Rapid preparation of nano lead sulfate-lead carbon black composite by microwave method as a negative electrode additive for lead-carbon batteries, Electrochim. Acta 384 (2021) 138411, https://doi.org/10.1016/j.electacta.2021.138411.
[16] Q. Li, C. Xu, L. Yang, K. Pei, Y. Zhao, X. Liu, et al., Pb/C composite with spherical Pb nanoparticles encapsulated in carbon microspheres as a high-performance anode for lithium-ion batteries, ACS Appl. Energy Mater. 3 (8) (2020) 7416–7426, https://doi.org/10.1021/acsaem.0c00812.
[17] W. Visscher, Cyclic voltammetry on lead electrodes in sulphuric acid solution, J. Power Sources 1 (3) (1976) 257–266, https://doi.org/10.1016/0378-7753(76)81003-8.
[18] S. Thangarasu, G. Palanisamy, S.-H. Roh, H.-Y. Jung, Nanoconfinement and interfacial effect of Pb nanoparticles into nanoporous carbon as a longer-lifespan negative electrode material for hybrid lead–carbon battery, ACS Sustain. Chem. Eng. 8 (23) (2020) 8868–8879, https://doi.org/10.1021/acssuschemeng.0c03461.
[19] D. Pavlov, P. Nikolov, T. Rogachev, Influence of expander components on the processes at the negative plates of lead-acid cells on high-rate partial-state-of-charge cycling. Part II. Effect of carbon additives on the processes of charge and discharge of negative plates, J. Power Sources 195 (14) (2010) 4444–4457, https://doi.org/10.1016/j.jpowsour.2009.12.132.
[20] J. Xie, Y. Hu, X. Wu, A. Ali, P. Shen, Positive effects of highly graphitized porous carbon loaded with PbO on cycle performance of negative plates of lead-acid batteries, Appl. Sci. (2021) 8469.